

# Supporting Material: The efficacy of aerosol-cloud-radiative perturbations in deep open- and closed-cell stratocumulus

Anna Possner<sup>1</sup>, Hailong Wang<sup>2</sup>, Rob Wood<sup>3</sup>, Ken Caldeira<sup>2</sup>, and Thomas P. Ackerman<sup>3</sup>

<sup>1</sup>Carnegie Institution for Science

<sup>1</sup>Pacific Northwest National Laboratory

<sup>1</sup>University of Washington

## 1 Figures

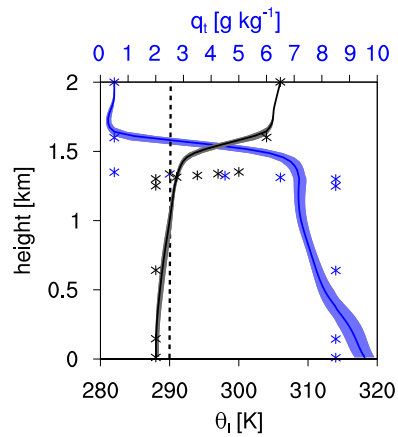


**Figure 1.** Simulated profiles of liquid potential temperature ( $\theta_l$ , black) and total moisture content ( $q_t$ , blue) for the *ctrl* simulation. Median and interquartile range of profiles are shown for the entire simulated period (45 h). Hence, the spread captures the entire spatio-temporal variability of both entities throughout the simulation. Dashed line indicates 290 K isoline. Markers denote prescribed sounding at initialisation for  $\theta_l$  (blue) and  $q_t$  (black).

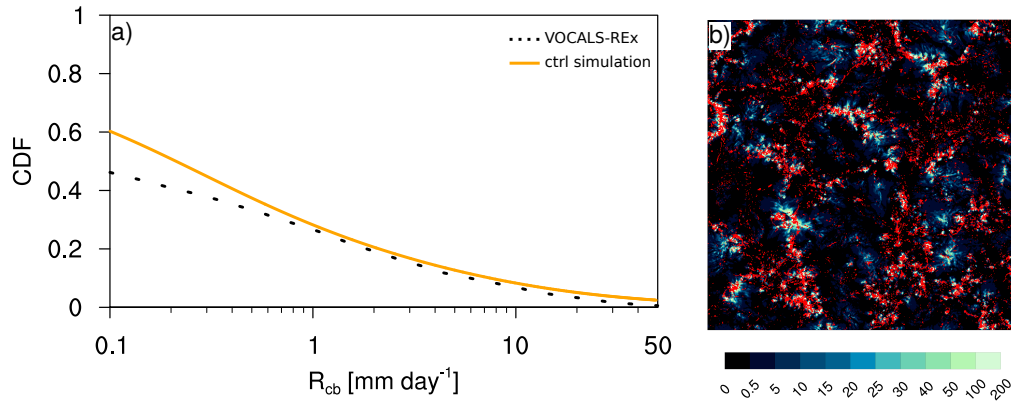


**Figure 2.** a) Cumulative distribution function (CDF) of cloud-base precipitation rate ( $R_{cb}$ ) obtained during campaign (Wood *et al.* (2011) denoted in black) and for VOCALS-REx simulations *ctrl* simulation (yellow). b) Cloud-base precipitation field ( $R_{cb}$ ) in contours with updraft regions (vertical velocity  $> 0.5 \text{ m s}^{-1}$ ) overlaid in red.

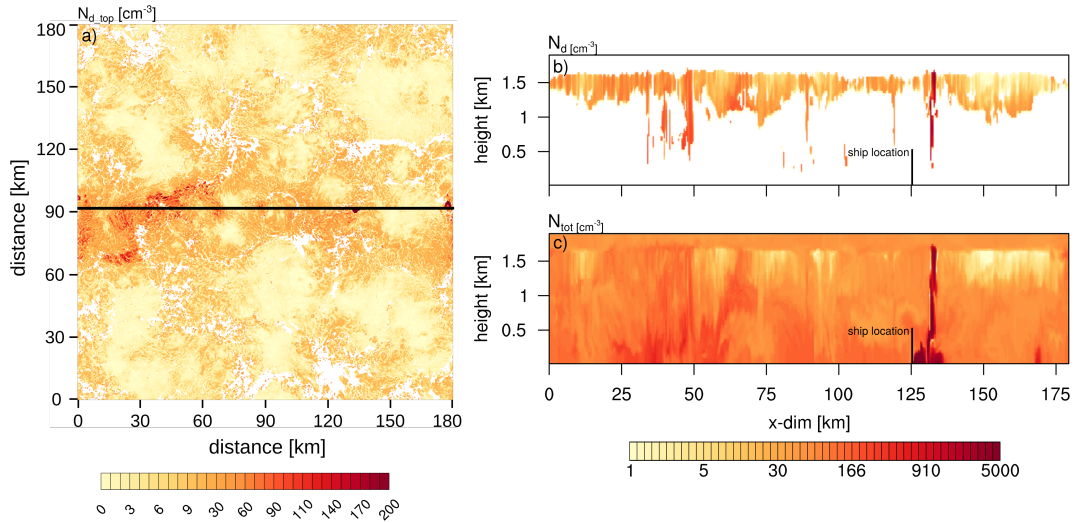


**Figure 3.** (a) instantaneous vertically integrated cloud droplet number concentration ( $N_d$ ) for ship\_open. Black line denotes location of cross-sections shown in b–c). (b)  $N_d$  and (c) total number concentration ( $N_{tot} = N_a + N_d$ , where  $N_a$  denotes the aerosol number concentration). Instantaneous location of ship is marked.

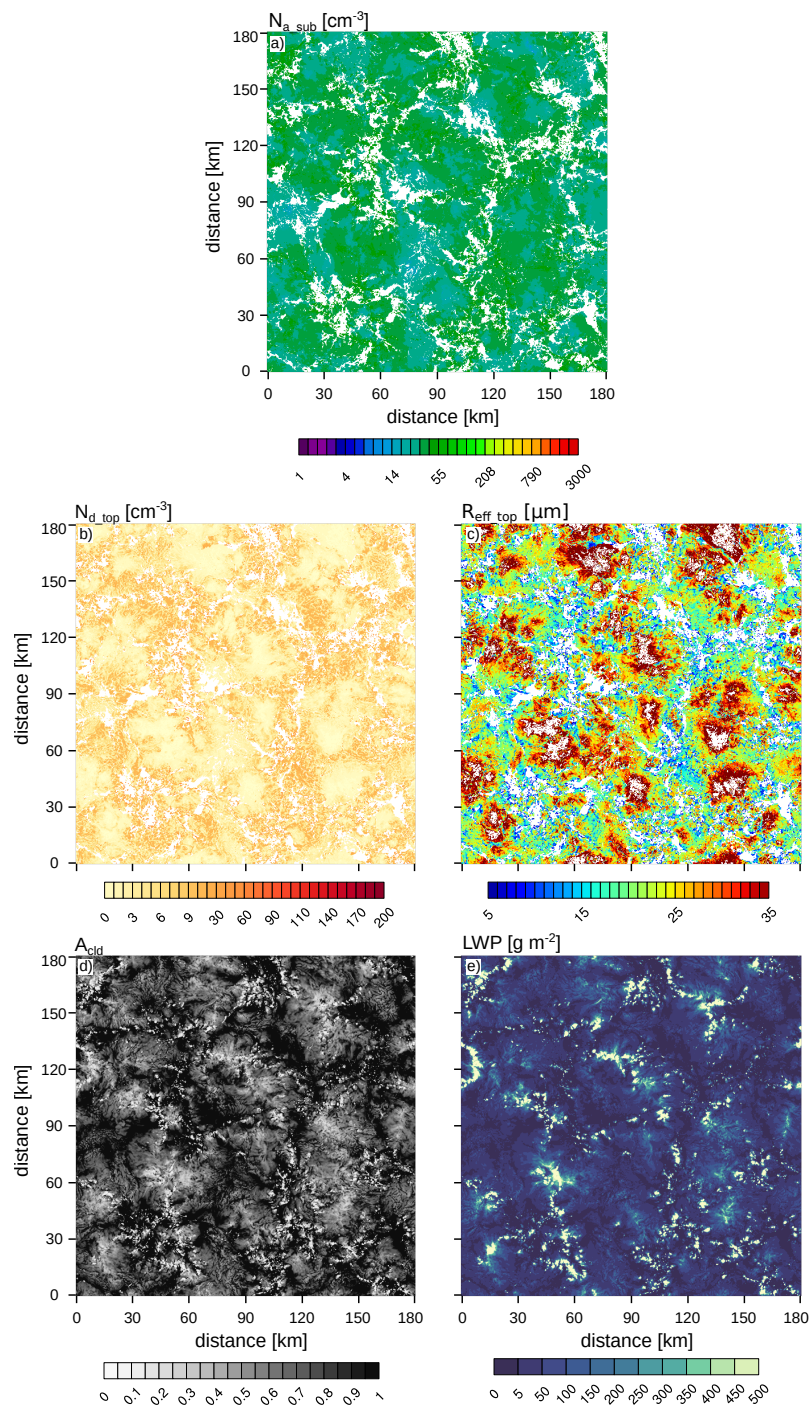


**Figure 4.** Same as Fig. 4 in manuscript, but for *ctrl* simulation.

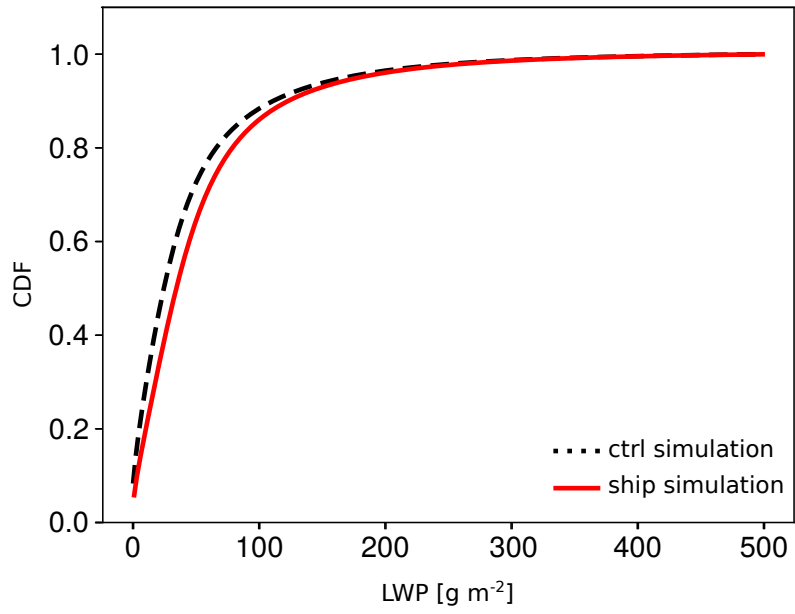


**Figure 5.** Cumulative distribution function (CDF) of liquid water path (*LWP*) for the *ctrl* and the *ship* simulation. CDF is computed over detrained cloud regions only over the last 24 h of both simulations.

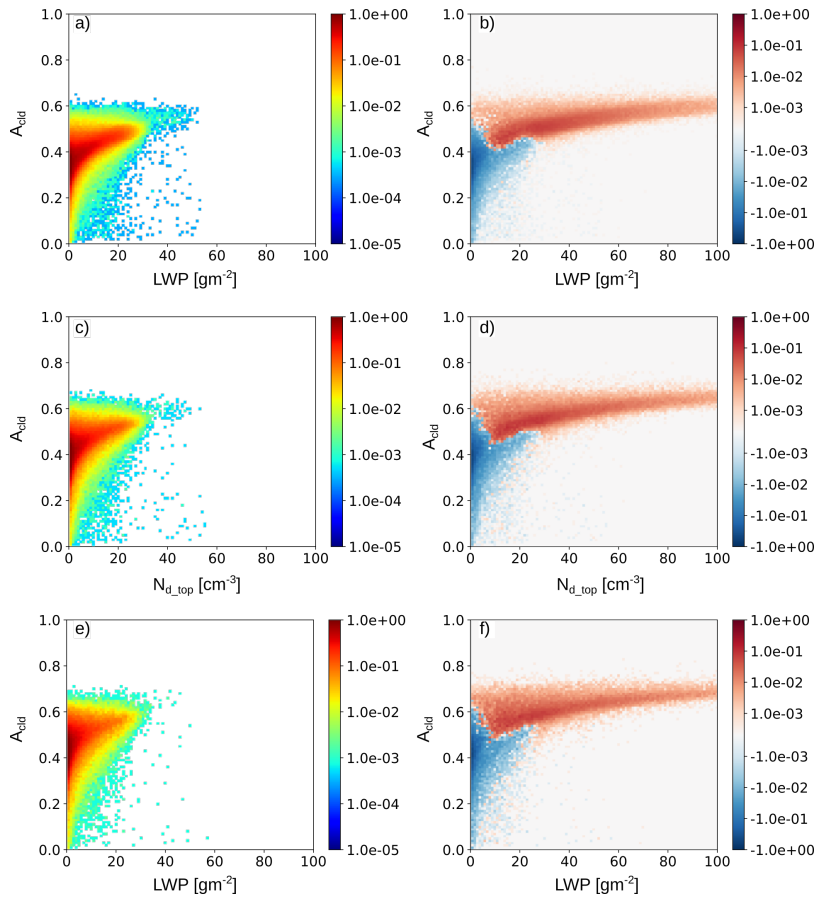


**Figure 6.** Occurrence rate  $F$  [%] for the cloud-top droplet number concentration ( $N_{d\_top}$ ) versus cloud albedo ( $A_{cld}$ ) phase space. The  $N_{d\_top}$ - $A_{cld}$  space was sub-filtered for  $LWP$  within the ranges of  $60-80 \text{ g m}^{-2}$  (top row),  $80-100 \text{ g m}^{-2}$  (middle row), and  $100-120 \text{ g m}^{-2}$  (bottom row). Results are shown in a,c,e) and for the last 24 h of the *ctrl* simulation and absolute changes in  $F$  for the *ship* simulation with respect to the *ctrl* simulation are shown in b,d,f). The bin widths for each of which  $F$  is defined are  $\Delta N_{d\_top} : 1 \text{ cm}^{-3}$ , and  $\Delta A_{cld} : 0.01$ .

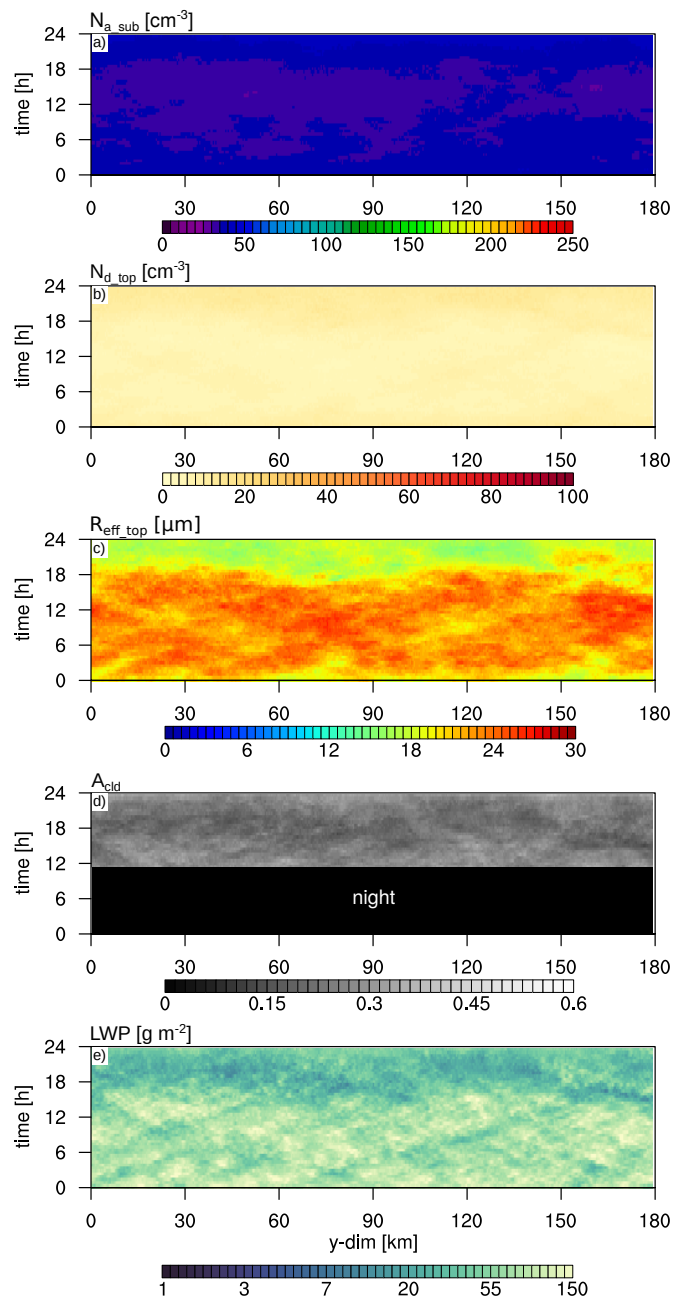


**Figure 7.** Same fields are shown as in Fig. 6 of manuscript, but for the *clean* simulation.